Pramāṇa - J. Phys., Vol. 35, No. 1, July 1990, pp. 49–65. © Printed in India.

A multi NaI(Tl) detector array for medium energy γ-ray spectroscopy

Y K AGARWAL, C V K BABA, D R CHAKRABARTY†, V M DATAR†, D A GOTHE, H C JAIN, A ROY and M K SHARAN

Tata Institute of Fundamental Research, Bombay 400005, India
†Nuclear Physics Division, Bhabha Atomic Research Centre, Trombay, Bombay 400085, India

MS received 12 March 1990

Abstract. An array of seven hexagonal NaI(Tl) detectors has been set up for measuring γ-ray spectra in the energy region $5\,\text{MeV} \leqslant E_\gamma \leqslant 40\,\text{MeV}$ with good accuracy. This is in contrast to earlier set ups which mostly used one large sized (about 10 inches $\phi \times 15$ inches long) NaI(Tl) detector. This set up has been made for the study of γ decay of GDR based on high spin states and ultra-dipole radiations.

The array has been provided with the following features: a) TOF discrimination against neutrons, b) pile up detection and elimination, c) active and passive shielding to cut down background and d) an array of trigger counters for multiplicity dependence measurements. The well known program EGS4 has been used to determine the response of the array for γ-rays in the energy region 5–40 MeV and several test measurements have been carried out to confirm the validity of the calculated response functions. Some typical γ-ray spectra from α and ^{16}O induced reactions measured at VECC, Calcutta and Pelletron accelerator at TIFR are also shown.

Keywords. 5–40 MeV gamma-ray; hexagonal NaI(Tl) detector array; time of flight; pile up; pulse shape discrimination; response; folding; unfolding.

PACS No. 29·4

1. Introduction

The study of high energy γ-rays from nuclear collisions has been of great interest in the last few years. These studies can broadly be classified into two categories. The first one is the study of gamma decay of isovector giant $E1$ resonance built on excited nuclear states. These photons are emitted in competition with other particles such as neutrons, protons and alphas, from an excited compound nucleus formed in low energy heavy ion collisions and shed light on nuclear structure, e.g. the shape evolution as function of spin, excitation energy etc. (Snover 1986; Gaardhøje *et al* 1984; Chakrabarty *et al* 1987a). Study of non-statistical or bremsstrahlung γ-ray emission in nucleus–nucleus collisions forms the second category. These γ-rays manifest themselves as an approximately exponential tail in the γ-ray spectrum for $E_\gamma > 20\,\text{MeV}$. Although the production mechanism of these hard photons is not well understood at present (Tam *et al* 1988; Nakayama and Berstch 1987), it is hoped that their study will enhance our understanding of the early phase of the collision. While there exist very many measurements of pre-equilibrium particle spectra, the presence of final state interactions with the residual nucleus makes their interpretation difficult. High energy photons are inherently clean probes and, because of their weak coupling to the nucleons, have a long mean free path in the nuclear medium.

Currently many types of γ detector assemblies are in use (Nifenecker and Pinston 1989). For $E_\gamma \geqslant 40$ MeV, the commonly used detector is the lead-glass Cerenkov detector (Stevenson *et al* 1986). This detector has a very poor response for low energy γ-rays. For $40\,\mathrm{MeV} \geqslant E_\gamma \geqslant 5\,\mathrm{MeV}$ and in cases where good energy resolution is desirable, inorganic scintillators [e.g. NaI(Tl), BGO (Murakami *et al* 1988), BaF_2 etc.] and/or solid state detectors are used. Recently a Ge detector (Gaardhøje *et al* 1988) also has been used to measure high energy γ-ray spectra. However, the small size of Ge detectors and the problems in using the cooled solid state detectors make any large scale use of these detectors for high energy γ-ray spectra measurements difficult. Most of the measurements of the γ decay of the GDR have been carried out using large detectors viewed by an array of photomultipliers. The following are some of the laboratories where such detectors have been set up: Frei University (Stolk 1988); KVI (Stolk *et al* 1989); Stony Brook (Chakrabarty *et al* 1987b); Seattle (Snover 1986) and Brookhaven (Sandorfi 1984). We have set up an array of hexagonal NaI(Tl) detectors and this turns out to be more flexible. The individual detectors can also be used separately (at different angles etc.) Also the problem of gain matching, uniformity etc. are less serious in this arrangement.

The present paper describes the NaI(Tl) detector array, which is being used for experiments at Variable Energy Cyclotron Centre (VECC), Calcutta and the 14 UD Pelletron accelerator at TIFR, Bombay. Various experimental aspects of the detector are described below in some detail; the results of the experiments will be presented elsewhere (Agarwal *et al* 1990).

A general description of the detector assembly, electronic and data collection system is presented in § 2.1. There are several essential features in such a set up. These are described in §§ 2.2–2.7.

a) neutron-gamma discrimination by time of flight (TOF) (§ 2.2); b) pile up detection (§ 2.3); c) pulse shape discrimination of neutron and gamma rays (§ 2.4); d) reduction of the background, mainly of cosmic ray origin (§ 2.5); e) the simulated and measured response of the detector (§ 2.6); f) a method for unfolding the measured spectrum to obtain the energy differential gamma ray cross-section (§ 2.7).

Finally, typical data from experimental runs at VECC and 14 UD Pelletron are presented in § 3. Some of the possible improvements in the set up will be briefly discussed in the end.

2. The detector set up

2.1 *General description of the detector*

The set up consists of 7 closely packed hexagonal NaI(Tl) detectors* each of length 15 cm and a hexagonal face of size 7·5 cm. The detector array was covered on the front and sides by ~ 1 cm thick layer of boric acid to reduce the thermal neutron background. Three plastic scintillators $50 \times 50 \times 5\,\mathrm{cm}^3$ each were placed on front, side and top to veto out cosmic ray events (see § 2.5). The NaI(Tl) detectors and plastic scintillator assembly were shielded against background γ-rays by a ~ 10 cm thick

* Obtained from Harshaw Chemie B V, De Meern, The Netherlands.

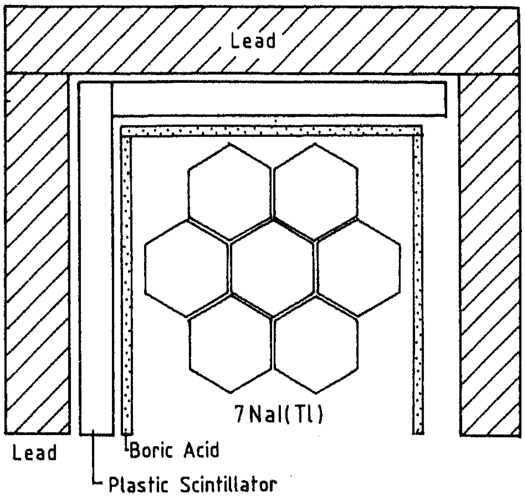

Figure 1. Schematic diagram of the front view of the set up; The NaI(Tl) detector array is surrounded by boric acid and 3 plastic scintillators which are placed on the side, top and front (not shown in figure). Lead bricks are placed on the side and the top.

layer of lead. A 5 mm thick lead sheet in front of the detector assembly was used to reduce the counting rate due to low energy gamma rays and X-rays produced in the target. The front lead sheet attenuates the intensity of the 15 MeV γ-ray by about 30%. In most experiments the detector assembly was placed at a distance of between 70 and 100 cm from the target providing a solid angle between 2 and 1% of 4π. Figure 1 shows the schematic diagram of the experimental set up.

Each NaI(Tl) crystal is canned in an aluminium container of wall thickness 3 mm and is viewed by a 7·6 cm ϕ HAMAMATSU R1911 photomultiplier tube (PMT). The energy information was obtained from the pulse taken from the 8th dynode. The dynode pulse from each detector was fed to a separate linear amplifier (for energy measurement) and a summing amplifier for pile up measurement (see § 2.3). The energy resolution of each detector was measured to be $\sim 8\%$ for the 662 keV line of ^{137}Cs. Careful gain matching of the pulse height was done for each detector, using a ^{60}CO source and the thermal neutron capture γ-ray in iodine in NaI(Tl) (6·83 MeV), during the experiment. The amplifier outputs were added in a summing amplifier, and used for recording the total energy deposited in the NaI(Tl) detector assembly.

The gain of the NaI(Tl) crystals can vary due to changes in count rate and ambient temperature. The gain matching for each detector was checked several times during the experiment, and it was found that the gains did not vary by more than 1%, for count rates of up to 100 kHz.

The anode pulse of the PMT was used for fast timing. In order to have a large dynamic range extending up to γ-ray energies of ~ 50 MeV, the photomultipliers were operated at a rather low voltage of 600–700 V. This required the use of fast timing amplifiers of gain 10. The amplified anode signal was then fed to a constant fraction discriminator (CFD) to generate a fast logic pulse. The triggering level in the CFD for these detectors was ~ 200 keV. The fast logic pulses from all the 7 NaI(Tl) detectors were delay matched to an accuracy of $< 0{\cdot}5$ ns and then fed to an OR circuit to provide the time singal.

In some of the experiments at VECC, data were also taken in coincidence with one or more of the four 5·1 × 5·1 cm ‘trigger’ NaI(Tl) detectors placed at a distance of

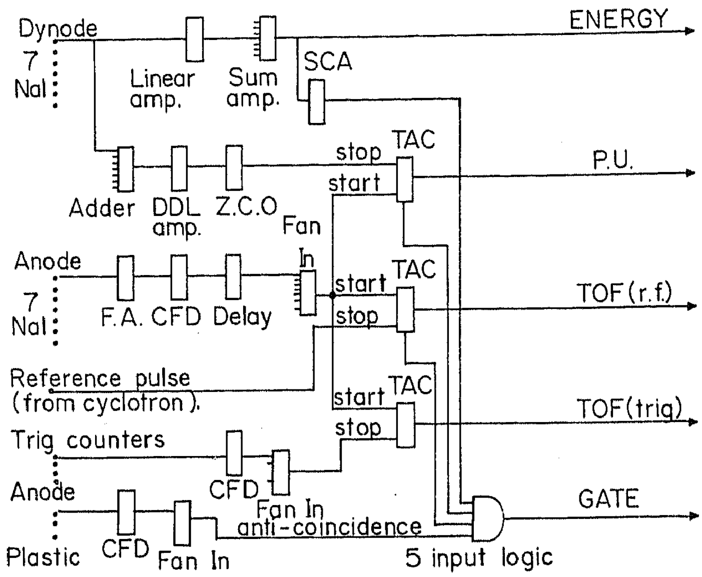

Figure 2. Block diagram of the electronics; at VECC, the data acquisition system based on NORD computer was used to collect four parameter list mode data, in coincidence with the 'GATE'.

~ 8 cm from the target. Such an experiment yields the mean multiplicity and hence the information about the angular momentum of the nucleus emitting a given high energy γ-ray. The anode pulses from these trigger detectors were sent to CFD's (threshold ~ 150 keV), matched in delay and sent through a fast multiplicity logic unit. The output of this multiplicity logic and the 'OR' output from the seven main NaI(Tl) detectors were fed to a time-to-analog converter (TAC), to obtain the time spectrum.

A block diagram of the electronics is shown in figure 2. The data were collected on a list mode basis. The parameters recorded were the total energy as discussed above, the time of flight with respect to beam r.f. [TOF(r.f.)] (see § 2.1), the timing between the trigger counters and the main detector [TOF(trig.)] and TAC output from the pile up detector (see § 2.3). The master gate was generated by a coincidence between the total outputs from the pile up TAC and TOF(r.f.) and an anti-coincidence from the veto detectors. The data rates are then very large for the list mode data recording and these were limited by further gating the master pulse by the output of a single channel analyser set to determine a low energy threshold. Typically data were taken for two thresholds. (1) 5 MeV for a short duration and (2) 8 MeV for a longer duration. The list mode data were later analysed off-line through sorting programmes. The spectra so obtained were combined using the energy region common in both the sets of data.

2.2 *n-γ discrimination*

Along with high energy γ-rays there is a large neutron flux incident on the detector, arising from the target as well as the beam dump. High energy γ-ray emission cross sections in nuclear collisions are typically 10^3–10^4 times smaller than neutron emission cross sections. These neutrons produce pulses in the NaI(Tl) detector through $(n, n'\gamma)$, (n, p), (n, α) and (n, γ) reaction in the scintillator material. The first three reactions are mainly from fast neutrons produced in the target. The last reaction is due to thermal neutrons (mainly from the beam dump), which get captured by ^{127}I in NaI(Tl) giving an energy pulse of 6·83 MeV, and the reaction is uncorrelated in time.

Since the high energy γ-ray yield is small, very good n-γ discrimination is essential.

This n-γ discrimination is achieved by the standard time of flight (TOF) technique. In this method, the detector assembly is kept at a suitable distance from the target and the time difference between a signal heralding a nuclear collision and another from the NaI(Tl) detector is a measure of the velocity of the interacting particle, which is 30 cm/ns for γ-rays and $\sim 1{\cdot}4\sqrt{E}$(MeV) cm/ns for non-relativistic neutrons.

In experiments at VECC, a pulse derived from the radio-frequency (r.f.) signal from the cyclotron was used as a timing reference. α beams of 50 MeV, had a beam bunch repetition time of 125 ns and bunch width of ~ 5 ns. At the 14 UD Pelletron, which provides D.C. beams, the timing reference signal was generated by a 5·1 cm $\phi \times 7{\cdot}6$ cm BaF_2 trigger detector placed at a distance of ~ 5 cm from the target. For the TOF measurement the TAC was started with the fast timing pulse from the NaI(Tl) array, and stopped by the reference signal suitably delayed.

The choice of the NaI(Tl) detector-target distance is a compromise between the necessity of having a reasonable solid angle in view of the small cross section involved and of having good n-γ discrimination even at the highest neutron energies. The time resolution of the NaI(Tl) array measured in coincidence with the trigger NaI(Tl) detector, using a ^{60}Co source was $\sim$4–5 ns. The time resolution for higher energy gamma rays ($E_\gamma \geqslant 8$ MeV), was found to be ~ 3 ns. The NaI(Tl) array was hence placed at a distance of > 70 cm from the target, giving a reasonable n-γ discrimination. The TOF spectrum shows a sharp peak due to γ-rays and a broad peak corresponding to neutrons of different energies. Both these peaks ride on a constant random background caused by thermal neutrons and cosmic rays.

The thermal neutron background arises mainly from the slowing down of fast neutrons originating in the beam dump. In experiments using α beams the background is particularly large, leading to a large pedestal in the TOF spectra. We have tried to minimize this background by moderating and capturing the fast neutrons in materials with high absorption cross sections, near the beam dump. The Faraday cup was surrounded by a tank of size $\sim 60 \times 60 \times 60\,\text{cm}^3$ containing a solution of boric acid in water. The beam pipe leading to the Faraday cup was surrounded by paraffin blocks and lined on the outside with lead bricks. A layer of boric acid surrounding the array reduced the thermal neutron background even further. The slow neutron contribution in the heavy ion experiments is much less because one can use a high Z material in the beam dump and because of the large specific energy loss of heavy ions in matter.

Figure 3 shows typical TOF spectra for three different energy gates. These spectra are from an experiment carried out at VECC. Figure 4 shows the spectra from an experiment at 14 UD Pelletron. It can be seen from these figures that with a target to detector distance of > 70 cm, a clean n-γ discrimination is obtained both with the VECC beam using the r.f. as a stop signal and in the DC beam at the Pelletron using a BaF_2 detector for a stop signal.

2.3 *Pile up measurement and elimination*

Pile up effects can occur in the spectra mainly due to the intense flux of neutron capture γ-rays ($\leqslant 7$ MeV) and also of low energy ($\leqslant 3$ MeV) γ-rays produced in the target. Two small pulses occurring within a time less than the amplifier shaping time can add and give a large pulse leading to a distortion of the high energy spectrum.

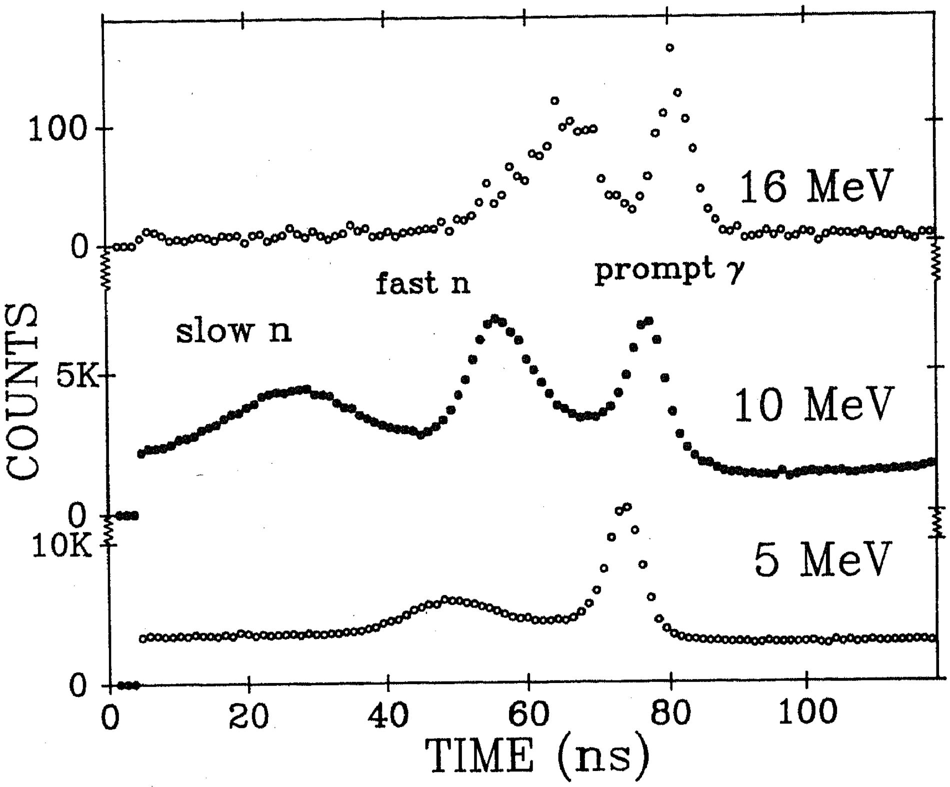

Figure 3. TOF(r.f.) spectra using 50 MeV α beam at VECC. The detector array was placed at a distance of 1 metre from the target. The three spectra shown correspond to the three energy windows shown in the figure.

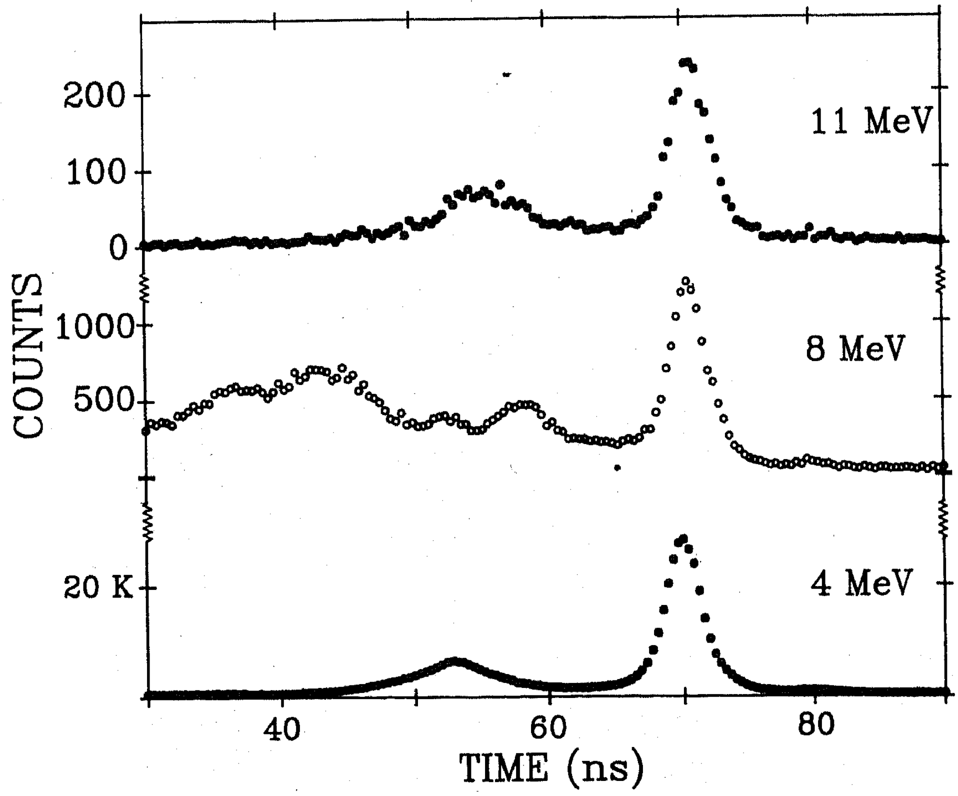

Figure 4. TOF(trig.) spectra for the experiment with ^{16}O at 14 UD Pelletron. The target-detector distance was 70 cm. The three spectra shown correspond to the three energy windows shown in the figure.

Detection and elimination of pile up events is very important, especially in pulsed beam measurements. For this purpose a suitable pile up eliminator was developed and used during the experiment.

The principle (Strauss 1963) of the pile up measurement is as follows: a doubly differentiated dynode pulse has a zero cross over (ZC/O) time independent of the pulse height but dependent on the rise time. In the event of a pile up between two pulses, the ZC/O time occurs later than that for an event in which there is no pile up. The difference in the cross over time depends on the time interval between the two pulses piling up. In our set up the dynode pulses of NaI(Tl) detectors were summed up and shaped using a double delay line (DDL) amplifier. Output of this unit was fed to a ZC/O trigger unit which generated a logic pulse when the DDL output crossed the base line. The timing of this pulse was measured with respect to the ORed CFD output by using a TAC. The TAC spectrum shows a peak corresponding to no pile up events and a tail due to pile up events (see e.g. figure 6). The TAC output was recorded event by event for pile up measurement or could be used for gating purposes for pile up rejection.

Figure 5 shows spectra of a ^{137}Cs source for a counting rate of 50 kHz, recorded in an individual NaI(Tl) detector. The spectrum without pile up rejection and that gated with a window on the 'no pile up' portion of the pile up TAC output are shown. The reduction at the low energy side of the pile up rejected spectrum is due to the cut off in the discriminator. A reduction in the pile up events is seen in the spectrum. However, a peak of double the pulse height of the 662 keV photo-peak still remains. This is caused by pulses occurring within the time window selected. In the actual experiment where list mode data were collected, this was corrected for in the off-line data analysis.

Figure 6 shows the pile up TAC spectrum from an experiment at VECC using 50 MeV α beam. The specrum has been projected for two energy gates 8–10 MeV and 10–15 MeV, taken in coincidence with a gate around prompt γ in TOF(r.f.). As can be seen the spectra have a cutoff on the lower side, a peak and a tail on the higher side arising from pile up of two pulses. The fraction of events in the tail is larger in the

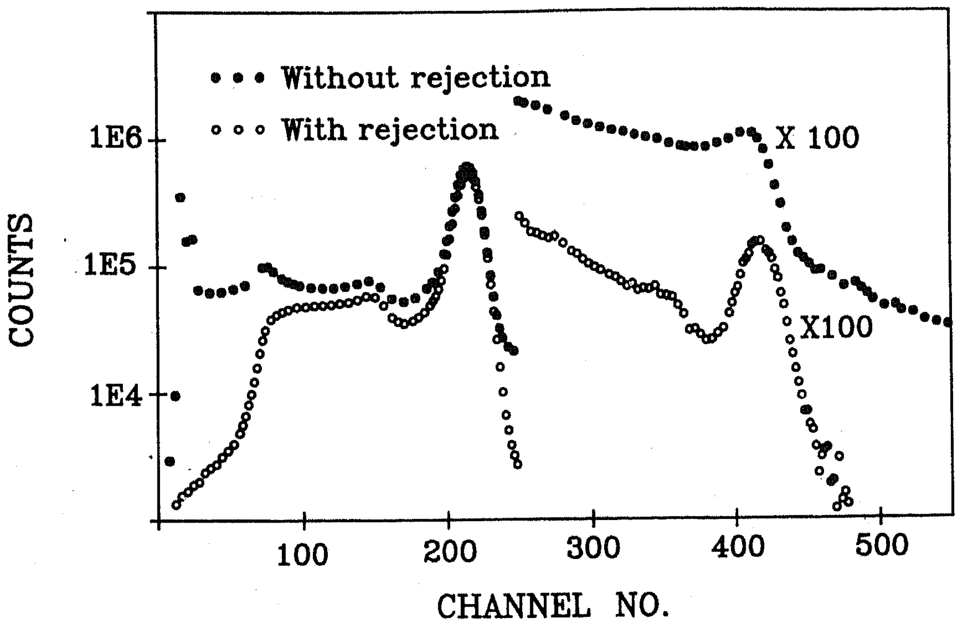

Figure 5. Pulse height spectra recorded in an individual NaI(Tl) detector using a ^{137}Cs source, with and without pile up rejection.

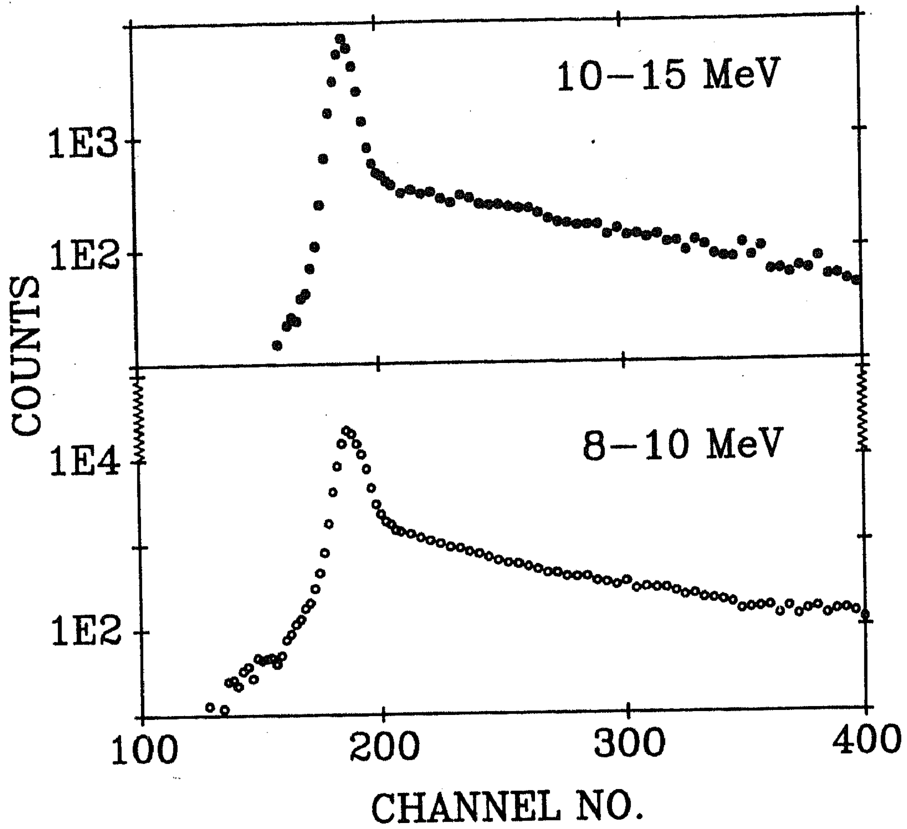

Figure 6. Typical pile up TAC spectra, recorded at VECC, for two energy windows 8–10 MeV and 10–15 MeV, taken in coincidence with a window around prompt γ.

8–10 MeV as compared to 15–20 MeV gated spectrum because of the pile up of the large flux of 6·83 MeV neutron capture γ-rays. The tail also increases with the total event rate. In the course of data analysis, a gate of $\sim$ 15 ns around the peak in the pile up spectrum was used to select non-pile up events, and a downward correction, which was energy dependent, arising from the presence of pile up events occurring within the time resolution of the pile up time spectrum, was applied. The efficacy of such a procedure was checked by comparing the γ-ray spectra in the $\alpha + Au$ run at $E_\alpha = 40$ MeV at two beam currents, with the target-detector configuration remaining the same, leading to singles counting rates of $\sim$20 kHz and $\sim$80 kHz in the γ-ray detector. The two γ-ray spectra obtained after sorting these two sets of data agreed to within 10% of each other. This procedure takes care of one more type of events which can result in wrong spectra: in some cases a neutron emitted in the same reaction can also reach the detector. The TOF will not reject this event but the pile up detector will.

2.4 *Pulse shape discrimination*

In addition to the TOF information which can be used to distinguish between neutrons and γ-rays, it is possible to use the pulse shape discrimination (PSD) properties of the NaI(Tl) scintillator to refine such an analysis. The PSD properties of many organic (Miller 1963) and inorganic scintillators, including NaI(Tl) (Bartle 1975; Doll *et al* 1989), are well known. The decay time of scintillation from a NaI(Tl) detector depends on whether the charged particle exciting it is an electron, proton, alpha etc. This decay time ranges from ~ 230 ns for electrons to ~ 190 ns for p, d etc., and determines the time difference between the start of the pulse and the ZC/O time. The pile up TAC output thus can not only be used to detect pile up, but also to discriminate between a γ-ray and a fast neutron event. The former produces mainly electrons and the latter mainly p and α in the primary interaction.

A typical plot of the pile up TAC spectrum for an energy window of 15–20 MeV is shown in figure 7. Also shown are the projections of the spectrum for the same energy bin and two TOF(r.f.) windows corresponding to neutrons and γ-rays. A complementary TOF(r.f.) projection with the same energy bin and two pile up TAC gates, corresponding to neutrons and γ-rays, along with the inclusive TOF(r.f.) spectrum is shown in figure 8. A comparison of these spectra clearly shows the n-γ discrimination property of the NaI(Tl) detector. Such a discrimination can be used for energies greater than ~ 10 MeV. By a judicious choice of a gate on the pile up TAC, the fast neutron contamination in the TOF(r.f.) gated γ-ray spectrum, which was estimated to be $\leqslant$ few per cent, was reduced by about a factor of three. Such a method was used when sorting data, obtained at VECC.

2.5 *Reduction of cosmic ray background*

The yield of high energy γ-rays in nuclear collisions, decreases roughly exponentially with γ-ray energy. For a reasonable target thickness and beam current, the count rate of γ-rays produced in nuclear reactions for $E_\gamma \geqslant 20$ MeV, becomes comparable to the cosmic ray background. The cosmic rays consist primarily of high energy muons and have a specific energy loss (dE/dx) $\sim 4{\cdot}8$ MeV/cm in NaI(Tl). The energy deposited in

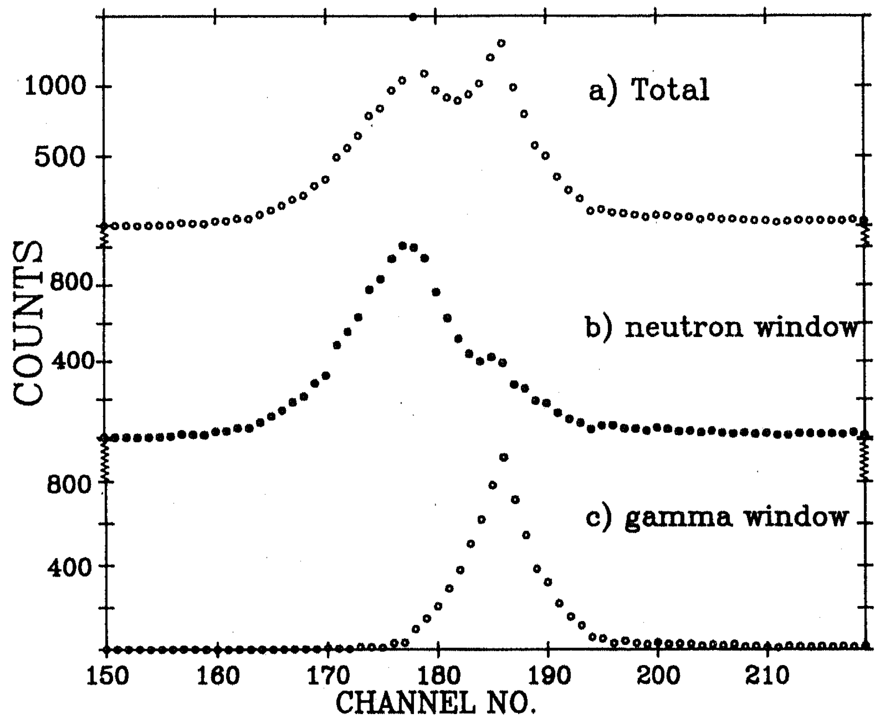

Figure 7. Pile up TAC spectra for energy window 15–20 MeV. **a)** Inclusive pile up spectrum for the above energy range; **b)** The spectrum in a) gated by neutrons (channel # 112–137) in the TOF(r.f.) spectrum (see figure 8); c) The spectrum in a) gated by γ-rays (channel # 141–158) in the TOF(r.f.) spectrum (see figure 8).

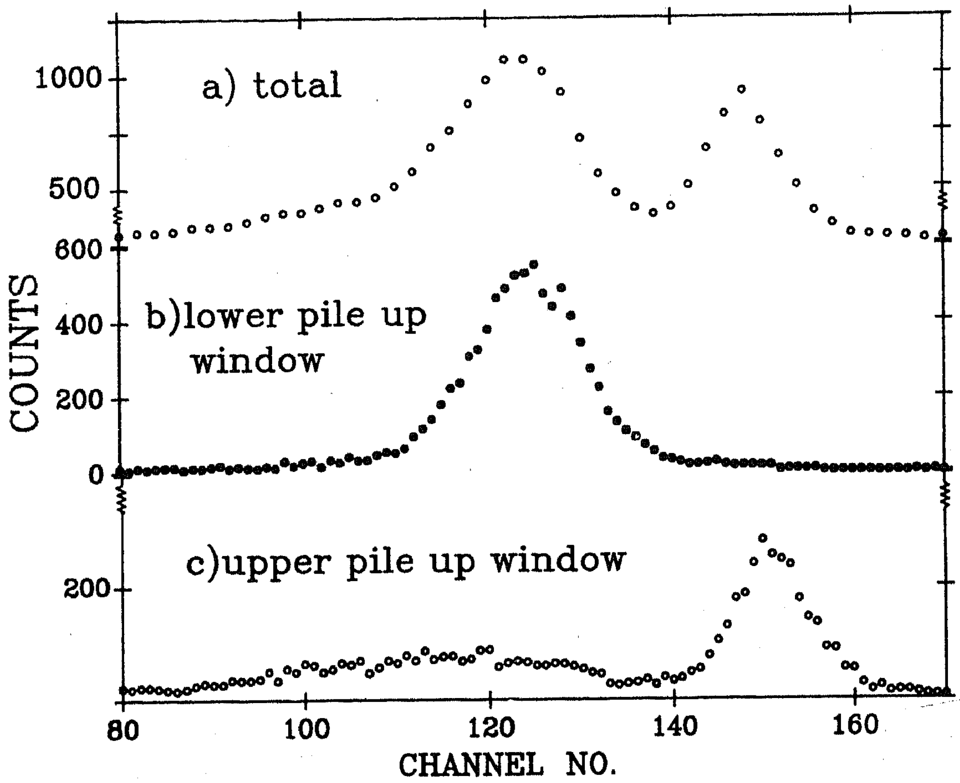

Figure 8. TOF(r.f.) spectra for energy window 15–20 MeV. **a)** Inclusive TOF(r.f.) spectrum; **b)** The spectrum in a) gated by a lower pile up window (channel # 160–186) in the pile up TAC spectrum (see figure 7); **c)** The spectrum in a) gated by a upper pile up window (channel # 187–200) in the pile up TAC spectrum (see figure 7).

our detector array depends on the length of detector material traversed and can be as high as ~ 200 MeV. Most of the muons penetrate the passive lead shielding around the detector and hence an active shield was used to reduce the cosmic ray background. The active shield consisted of three rectangular plastic scintillators (made in the Chemical Engineering Division, BARC) of dimensions $50 \times 50 \times 5\,cm^3$ each. A perspex light guide in the form of a truncated triangle (50 cm base × 40 cm height) was optically coupled to one side of each plastic scintillator. The narrow end of the light guide was optically coupled to a fast 5 cm ϕ photomultiplier (RCA 8575). The whole assembly was enclosed in a light tight aluminium box. The anode pulse from each of the photomultipliers was fed to a quad CFD whose triggering level was set at ~ 1 MeV. The CFD outputs from each of the three plastic scintillators were mixed in a FAN IN unit and the output pulse was used to veto events in the NaI(Tl) detector array. A typical background spectrum in the NaI(Tl) detector array with and without the cosmic ray veto and also with and without the passive lead shielding is shown in figure 9. One can see that the lead shield is more effective for low γ energies whereas for high energies the active shield is better. With such an arrangement a background reduction of ~ 5 was obtained at an energy of ~ 20 MeV. This is not as good as reported for other high energy γ-ray detector set ups and is limited by the quality of the plastic scintillator. In actual experiments, the energy spectrum is gated by a window (~ 10 ns wide) of the TOF(r.f.) and/or TOF(trig.). Such a gating brings in a reduction by further factors of ~ 12 in the former case and ~ 100 or more in the latter case. Thus in practice, the

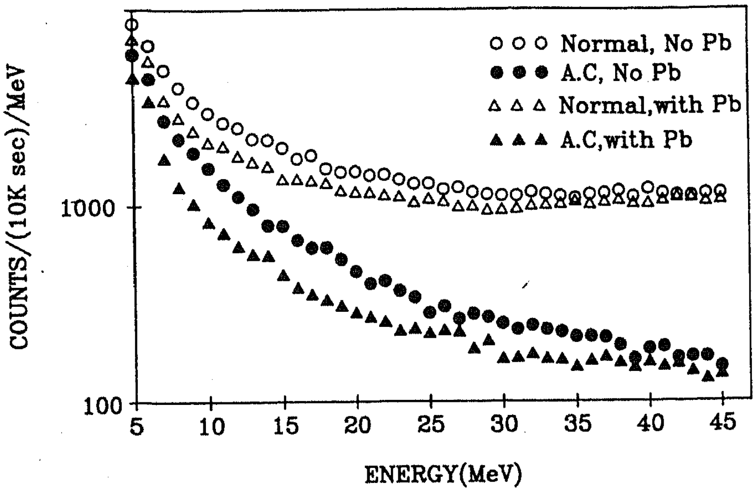

Figure 9. Cosmic ray background spectra measured in the NaI(Tl) detector array. Spectra with different conditions of active and passive shielding are shown.

spectrum up to ~ 30–35 MeV can be recorded without a comparable contribution from the cosmic ray background.

2.6 *Detector response: measurement and simulation*

When a high energy γ-ray ($E_\gamma \geqslant 5$ MeV) is incident on a NaI(Tl) detector the dominant process of interaction is e^+e^- pair production. This develops into an electromagnetic shower which consists of e^+e^- pairs and low energy photons. For proper spectroscopy the full shower must be confined in the detector. In a small sized detector, a significant fraction of the shower escapes, resulting in a reduced full energy peak efficiency and a tail on the lower side of the full energy peak. In our detector configuration, we sum up the energy deposited in each of the seven NaI(Tl) detectors so that, effectively, we have one large sized detector. This gives a much better relative full energy peak efficiency compared to that for an individual detector, as can be seen in figure 10.

Since the response of the NaI(Tl) detector array to an incident mono-energetic γ-ray depends on its energy, ideally one must measure the response over the energy region of interest which in our case is ~ 5–40 MeV. This is required either in folding theoretical γ-ray spectra for comparison with experiment or in unfolding measured spectra to give energy differential cross sections. Typically one requires detector response functions for 1 MeV increments in γ-ray energy. As this would take an enormous amount of beam time, the usual practice, which we have also followed, is to compare the measured response with a Monte-Carlo computer simulation at a few energies spanning the range of interest. If the simulated and measured spectra agree within errors, the simulated response over the γ-ray energy region of interest can be used and relied upon.

The computer code EGS4 (electron-gamma shower code, version 4) (Nelson *et al* 1985) was used for the response simulation. This code uses the Monte Carlo method to simulate the electromagnetic shower in the detector material. The relevant output of the EGS4 code is in the form of a spectrum of the energy deposited in the NaI(Tl) detector. This has to be folded with the finite energy resolution of the detector. A Gaussian function, with a width corresponding to a FWHM (MeV) varying as $0{\cdot}1(E_\gamma/1\,\text{MeV})^{1/2}$ was used for this purpose. Due to the statistical nature of the code, the

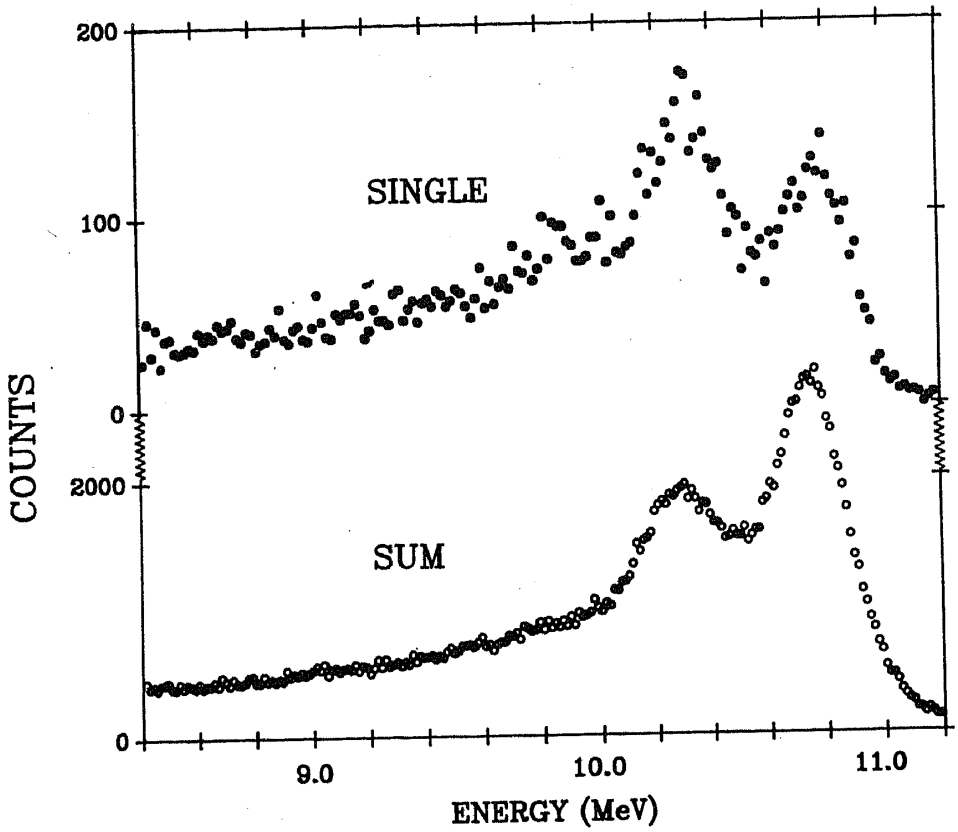

Figure 10. Measured line shapes for the 10·76 MeV γ-ray produced in the $^{27}Al(p,\gamma)^{28}Si$ reaction, *single* detector alone, and for all the detectors *summed* together.

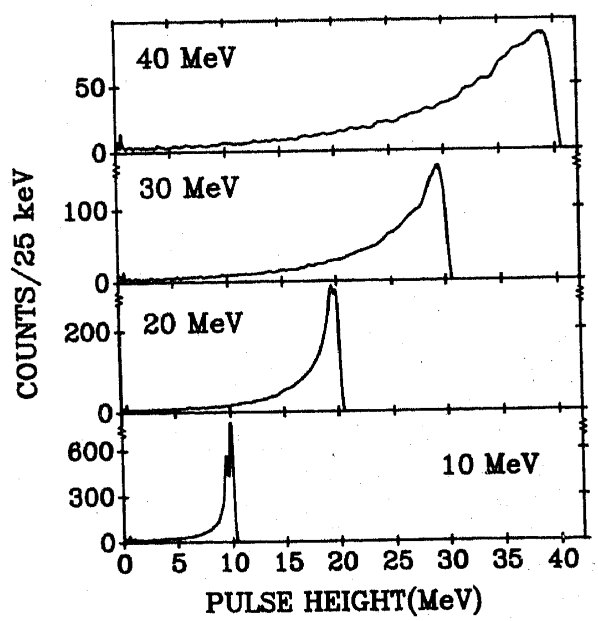

Figure 11. Calculated response of the 7 NaI(Tl) detector array to monochromatic γ-rays of different energies. The full energy peak and the escape peaks can be recognized. The fluctuations in the spectra are because of finite number of events run in the Monte Carlo simulation program.

accuracy of the simulation depends on the number of events sampled. Typically 100,000 events were run on the CYBER computer at TIFR. Figure 11 shows the result of such a simulation for γ-ray energies 10, 20, 30 and 40 MeV incident on the detector array. These calculated response functions were compared with measurements carried out at the 5·5 MV Van de Graaff accelerator at BARC and the Pelletron accelerator at TIFR for a few energies.

The reaction $^{27}Al(p,\gamma)^{28}Si$, which has a resonance at a proton energy of 992 keV, was used to measure the detector response for 10·76 MeV γ-rays. The thick target yield of this γ-ray per incident proton is well known (Antilla *et al* 1977). The measured γ-ray spectrum agreed with the calculated response in both shape and magnitude to within 10%, as can be seen in figure 12. The $^{11}B(p,\gamma)^{12}C$ reaction at a proton energy of 1·4 MeV was used to measure the response at γ-ray energies of 17·27 and 12·84 MeV. Here too the agreement between the measured response and the EGS4 simulation is reasonably good (see figure 13). One more test measurement with 14 MeV protons incident on a boron target was carried out at the Pelletron. The response for the 24·4 MeV and 28·8 MeV γ-rays measured was found to be in good agreement with the results of EGS4 calculations for these energies.

The good agreement between calculated and measured response of the NaI(Tl) detector array in the γ-ray energy regions 6·14 MeV to 28·8 MeV, gives us the confidence in using the simulations in the energy range 5–40 MeV.

2.7 *Unfolding of experimental cross section*

The shape of the measured spectrum is different from the actual spectrum of γ-rays incident on the detector array. This is because the detector response function which folds the original γ-ray spectrum is not a delta function. In order to derive the original spectrum one has therefore to unfold the measured γ-ray spectrum.

In many high energy γ-ray measurements, a theoretical spectrum (e.g. that

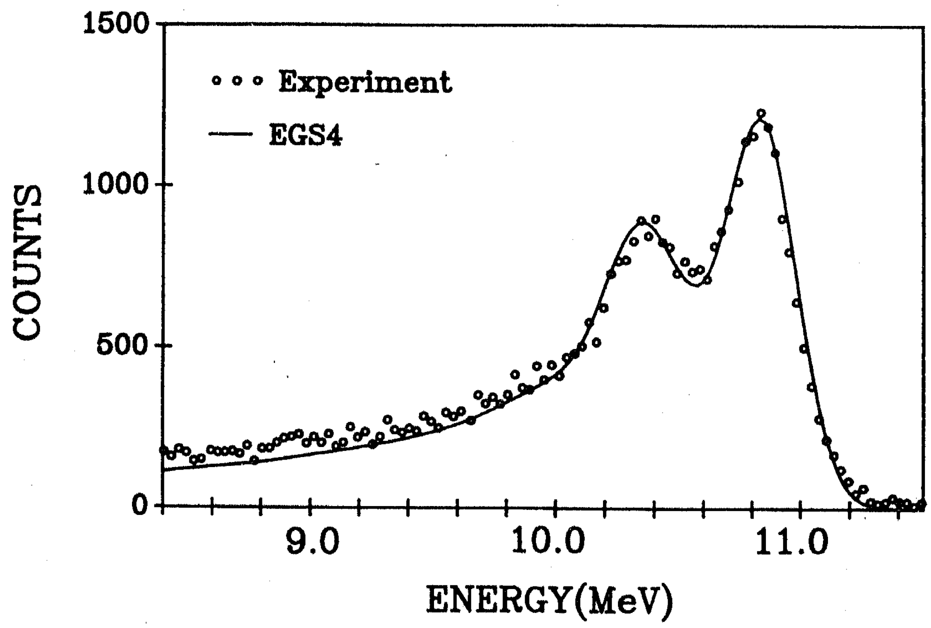

Figure 12. Calculated and measured response of the detector array to 10·76 MeV γ-ray in the $^{27}Al(p,\gamma)^{28}Si$ reaction.

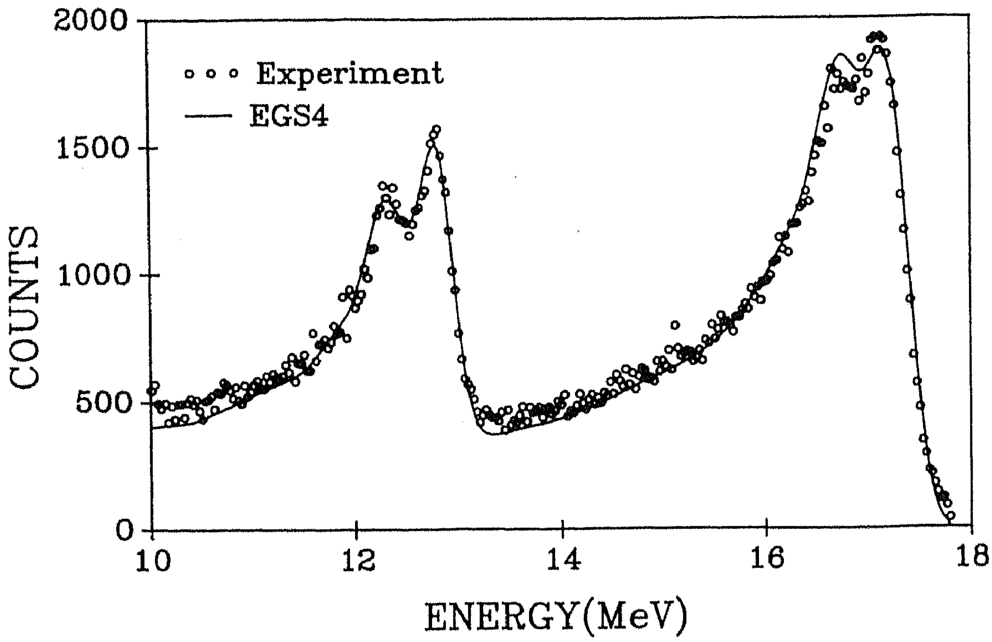

Figure 13. Calculated and measured response of the detector array to 17·27 MeV and 12·48 MeV γ-ray, produced in the reaction $^{11}B(p,\gamma)^{12}C$.

calculated from a statistical code) is folded with the detector response function, for comparison with measured spectra. However, in the case of γ-rays beyond the giant dipole resonance, even the mechanism of photon production is uncertain. It is more meaningful therefore to unfold the measured spectrum to obtain the differential cross section so that they may be compared with the predictions of various models.

The measured spectrum $G(E_\gamma)$ can be written as

$$G(E_\gamma) = N\int R(E'_\gamma, E_\gamma)F(E'_\gamma)\mathrm{d}E'_\gamma$$

where $F(E'_\gamma)$ is the energy differential cross section and R is the response function and N is the normalization constant, calculated from the target thickness, beam current etc. There are two methods of deriving $F(E'_\gamma)$ from $G(E_\gamma)$ namely the matrix inversion method and the iterative method. In the former method the integral is discretised so that the problem reduces to one of inverting the matrix $R(E'_\gamma, E_\gamma)$. However if the discrete step size is to be small, which is necessary for accuracy, the dimension of the matrix becomes very large, particularly when one has a γ-ray spectrum extending up to ~ 40 MeV. This however is not unmanageable. In the latter method any proposed cross section function $F^0(E_\gamma)$ is the starting point. This may be chosen to be a statistical model prediction or a sum of two exponentials depending upon the spectrum shape. This cross section is then folded with the response function with a very small step (~ 50 keV) in the numerical integration involved. The folded cross section, after multiplying by proper constants (consistent with the beam charge, target, thickness, detector solid angle, front absorption etc.) is compared with the measured spectrum. The new set of the proposed cross section for different γ energies is then obtained from the old one by multiplying at each experimental point by the ratio of the measured and calculated yields, and the whole procedure is repeated. This iterative process converges if the experimental yield is smoothly varying with energy. A practical difficulty in both these methods arises from the statistical fluctuations

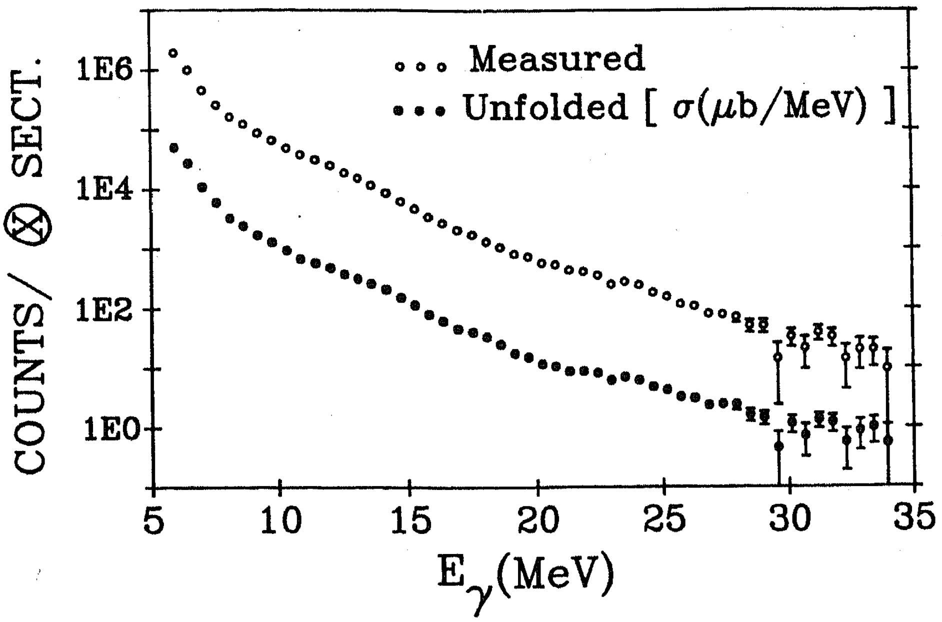

Figure 14. Measured γ-ray spectrum for the reaction $\alpha + {}^{197}\mathrm{Au}$ at $E_\alpha = 50$ MeV. The unfolded cross-section was calculated as discussed in the text.

present in the data especially at high γ energies. These give rise to damped oscillations in the unfolded cross section on the lower side of a single point which might lie outside the smoothly falling spectrum. In regions of low statistics one gets an even more fluctuating derived cross section. Since we are unaware of the solution to this problem we have followed a different procedure for unfolding.

We first create a dummy experimental spectrum by drawing a smooth line through the data points. This is unfolded by using the iterative procedure discussed above and finally the unfolded cross section is multiplied by the ratio of the actual and the dummy data at each experimental point. The errors are calculated by demanding the same fractional values as in the original spectrum. It should be emphasized again that this procedure only ensures that folding of smoothened unfolded cross section will give smoothened experimental data. Figure 14 shows an example of the above unfolding process.

3. Results and possible improvements of the set up

Two examples of measured γ-ray spectra in the reactions, $\alpha + {}^{197}\mathrm{Au}$ at $E_\alpha = 50$ MeV and ${}^{16}\mathrm{O} + {}^{181}\mathrm{Ta}$ at $E\,{}^{16}\mathrm{O} = 85$ MeV are shown in figure 15. The ${}^{197}\mathrm{Au}$ spectrum has been projected out of data, taken in a multiparameter mode, after cuts on the TOF(r.f.) and pile up TAC, subtraction of thermal neutron and cosmic ray background and correction for the residual pile up events. The Ta data on the other hand has been derived from a 2 parameter E_γ-TOF(trig.) measurement in which a hardware window was set on the pile up TAC output. Although the compound nuclei produced in the α and ${}^{16}\mathrm{O}$ bombardments (${}^{201}\mathrm{Tl}$ and ${}^{197}\mathrm{Tl}$ respectively) have approximately the same excitation energy, the γ-ray spectra have very different shapes. The latter can be fitted within a statistical model incorporating the giant dipole γ-ray strength function. The

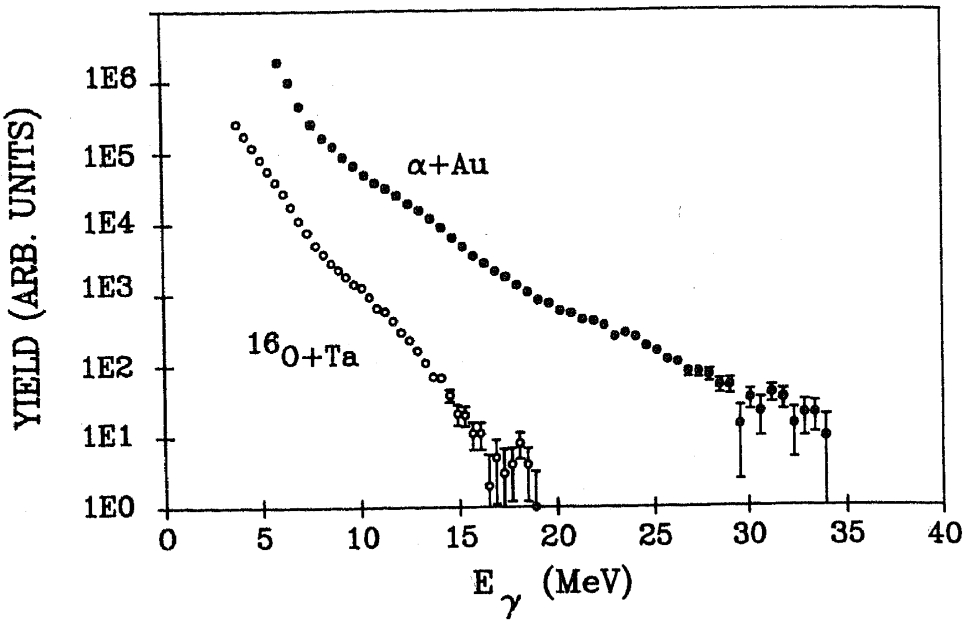

Figure 15. Measured γ-ray spectrum with 50 MeV α and 85 MeV ^{16}O beams, incident on Au and Ta respectively.

former, however, has a large 'ultra dipole radiation' tail, which will be discussed elsewhere (Agarwal *et al* 1990).

As discussed earlier, increasing the detector size is advantageous for high energy γ-ray spectroscopy. We intend to set up another array with 7 closely packed hexagonal NaI(Tl) detectors of length 25 cm. The whole array will be surrounded by a better quality annular plastic scintillator which will be further shielded by lead rings around the active plastic shield. Such a set up would be compact and give better efficiency for high energy γ-rays, along with improved cosmic background reduction and enable measurements of small yields and search for phenomena like γ-ray decay of giant quadrupole resonance, ultradipole radiations etc.

Acknowledgements

The authors wish to thank Prof. W R Nelson of Stanford University for providing us a copy of the code EGS4. Thanks are also due to the operators at the three accelerators: Van de Graaff accelarator at BARC, Trombay, Bombay, the 14 UD Pelletron accelarator at TIFR, Bombay and the Variable Energy Cyclotron Centre, Calcutta for providing the beams used for the various measurements presented here. We also wish to thank Shri M T Gaikwad for efficiently taking care of the various workshop jobs which were necessary to get the set up operational.

References

Agarwal Y K *et al* 1990 (to be published)
Antilla A, Keinonem J, Hautala M and Forsblom I 1977 *Nucl. Instrum. Methods* **147** 501
Bartle C M 1975 *Nucl. Instrum. Methods* **124** 547
Chakrabarty D R, Thoennessen M, Alamanos N, Paul P and Sen S 1987a *Phys. Rev. Lett.* **58** 1092

Chakrabarty D R, Sen S, Thoennessen M, Alamanos N, Paul P, Schicker R, Stachel J and Gaardhøje J J 1987b *Phys. Rev.* **C36** 1886
Doll P, Fink G, Haupenthal M, Finlay R W, Hauber S, Klages H O, Schieler H, Smend F and Wicke G D 1989 *Nucl. Instrum. Methods in Phys. Res.* **A285** 464
Gaardhøje J J, Ellegaard C, Herskind B and Steadman S G 1984 *Phys. Rev. Lett.* **53** 148
Gaardhøje J J, Bruce A M and Herskind B 1988 *Nucl. Phys.* **A482** 121C
Miller T G 1963 *Nucl. Instrum. Methods* **63** 121
Murakami T, Kasagi J, Yoshida K, Harada H, Tachibanaki H, Kubono S, Yasue M, Tanaka M H, Lee S M, Ogiwara M, Fujiwara H and Jeong S C 1988 (unpublished)
Nakayama K and Bertsch G F 1987 *Phys. Rev.* **C36** 1848
Nelson W R, Hirayama H and Roger D W O 1985 Stanford University Report SLAC-265
Nifenecker H and Pinston J A 1989 *Progress in particle and nuclear physics* **23** 271
Sandorfi A M 1984 *Heavy ion science* (ed.) D Allen Bromley (New York, London: Plenum Press) vol. 2
Snover K A 1986 *Annu. Rev. Nucl. Part. Sci.* **36** 545
Stevenson J, Beard K B, Benenson W, Clayton J, Kashy E, Lampis A, Morrissey D J, Samuel M, Smith R J, Tam C L and Winfield J S 1986 *Phys. Rev. Lett.* **57** 555
Stolk A 1988 Ph.D. Thesis Vrije Universiteit, Amsterdam
Stolk A, Hesselink W H A, Hofmann H J, Noorman R F, van Schagen J P S, Sujkowski Z, Verheul H, de Voigt M J A and Witte D J P 1989 *Phys. Rev.* **C40** R2454
Strauss M G 1963 *Rev. Sci. Instrum.* **34** 335
Tam C L, Stevenson J, Benenson W, Clayton J, Chen Y, Kashy E, Lampis A R, Morrisey D J, Samuel M, Murakami T K and Winsfield J 1988 *Phys. Rev.* **C38** 2526